HEFAT2014
10th International Conference on Heat Transfer, Fluid Mechanics and Thermodynamics
14 – 26 July 2014
Orlando, Florida

AN INVESTIGATION OF TEMPERATURE SEPARATION PHENOMENON IN THE VORTEX CHAMBER

A Ran Ye[1*], Vincent Lijo[2], Toshiaki Setoguchi[3] and Heuy Dong Kim[1]
[1]Department of Mechanical Engineering, Andong National University, Korea
[2]Fluid Machinery Technology & Research Centre, Daejoo Machinery Co. Ltd., Korea
[3]Saga University, Saga-shi, Saga, Japan
*Author for correspondence E-mail: aranye@anuis.andong.ac.kr

ABSTRACT

The vortex chamber is a simple device with no moving parts that separates compressed gas into a high temperature region and a low temperature region. Recently, vortex chamber is being received much attention but also high industrial demand because of its structural simplicity and better performance of the temperature separation, compared with the previous vortex tubes. In the present study, both experimental and numerical analysis has been carried out to investigate the temperature separation inside a vortex chamber. Working fluid enters the chamber through four tangential inlet ports and exits through one central exit port. To investigate the temperature separation phenomenon, static pressures and temperatures at several points inside the vortex chamber were measured using highly sensitive pressure transducers and thermocouples. Data obtained from experiments was used to verify the computational results. 3-D unsteady RANS equations were considered to simulate compressible flow inside the vortex chamber. Numerical results were observed to be in good agreement with experimental ones. Many hypotheses are discussed in terms of energy transfer mechanisms and Pressure Gradient Waves (PGW) in the paper.

INTRODUCTION

The vortex chamber is a simple device that separates compressed gas into a high temperature and a low temperature. The vortex chamber is made of a cylindrical camber in which gas is injected tangentially. Passing through the vortex chamber, injected gas forms strong vertical flow in the chamber, which moves from the periphery to the center of the vortex installation. The resulting flow creates strong vertex flow, which has been obtained an outward radial high temperature region and an inner low temperature one. The vortex tube has been used of low-temperature gas, but the vortex chamber is a possibility of application to the engineering field to be used as a hot section.

As typical application of this phenomenon, there is a vortex tube. The vortex tube was suggested for the first time by J. Ranque[1], R. Hilsch[2] designed and produced the tube to carried out the experiment. Since then, the vortex tube has been known as Ranque vortex tube (RVT), Hilsch Vortex tube (RHVT) and Ranque-Hilsch vortex tube (RHVT).

Recently, according to an experimental study by Beliavsky[3], when pressurized air with room temperature is supplied to the vortex chamber, the highest temperature of periphery was 700 K, and the lowest temperature of the central zone was 250 K. Also he introduced the concept of pressure gradient wave to explain the temperature separation phenomenon [4]. If such high temperature separation is possible, it could be beneficial to study the temperature separation in a vortex chamber.

Vortex chamber is structurally simpler and more efficient in terms of the temperature separation than the RHVT. However, the fluid dynamic and thermodynamic processes are extremely complex. RHVT is well-studied [5-8] to understand temperature separation phenomenon. Currently there is no conclusive evidence as to the mode of temperature separation within a vortex chamber. Hence, systematic study is conducted to explain the temperature separation phenomenon in a vortex chamber.

In this study, CFD analysis of the vortex chamber has been carried out to simulate the flow pattern, thermal separation, pressure gradient etc. so that they are comparable with the experimental results.

NOMENCLATURE

D	[m]	Vortex chamber diameter
d	[m]	Outlet diaphragm diameter
H	[m]	Vortex chamber height
h	[m]	Distance from low dis to central rod
r	[m]	Radius
T	[K]	Temperature
A	[m^2]	Area normal to radius

Subscripts

exit	Exit
out	Out
0	Atmospheric condition

c	Hot thermocouple location
i	Cold thermocouple location
25	Position on the lower disc at a diameters of 25mm
50	Position on the lower disc at a diameters of 50mm
70	Position on the lower disc at a diameters of 70mm

EXPERIMENT SETUP

Carrying out experimental studies is significantly complicated mainly due to the rapid rotating flows present inside the vortex chamber. Introduction of any measuring sensors into the vortex chamber can lead to flow distortion. The geometry used for this study is identical to the vortex chamber used in our recent experimental work [9]. It consisted of the following components: tangential nozzle attached vortex chamber a straight circular tube shape, the outer edge of the vortex chamber, a rod which is mounted on the central axis of the vortex chamber and a collector. The cylindrical cavity (hot-end plug) has 8 mm diameter and a depth of 32 mm. The schematic diagram of the vortex chamber is shown in Fig .1. in this the chamber diameter D is 140 mm, height H = 25 mm, distance of rod from the lower disc h = 10 mm. Atmospheric pressure (P_0) and temperature (T_0) are 101.2 kPa and 283 K respectively.

Compressed air is supplied to the vortex chamber through four tangential nozzles. During the experiment, the pressure ratio P/P_0 was increased to 6 in increments of 1 stepwise by using a motorized valve. Symbol of ●, x is location for high-sensitive thermocouples and pressure transducers. The pressure readings were measured by transmitters (Kulite Co. : XT-190) The temperature readings were measured by thermocouples (CHINO Co. : SUS316).

NUMERICAL METHOD

The computational model is taken from experimental model to investigate the 3-D unsteady compressible flows inside the vortex chamber. The geometry modeling and meshing is done using ICEM-CFD as showed in Fig 2. Grid dependency study has been conducted and the computational domain consists of 1.3 million elements. Near wall features are captured by putting very fine prism layers attached to the walls.

A commercial software ANSYS CFD is used to conduct computational analysis using the computational model above. At the outlet, static pressure of 101.2 kPa is specified and the stagnation pressure at the nozzle inlet is 415 kPa. The inlet total temperature is kept constant at 283 K throughout this process. The walls are specified as adiabatic. The operating fluid used for the simulation has been selected as air. The turbulence model selected for the present investigation is Realizable k-ε and the time step used is 1×10^{-6} s.

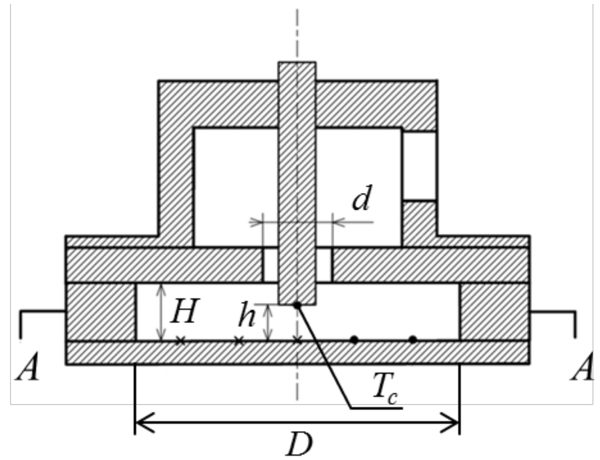

(a) Cross-sectional front view

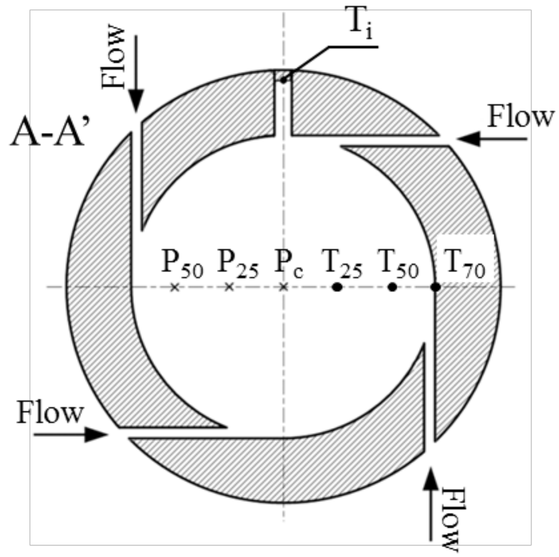

(b) Cross-sectional top view

Figure 1 Schematic of vortex chamber with a cavity

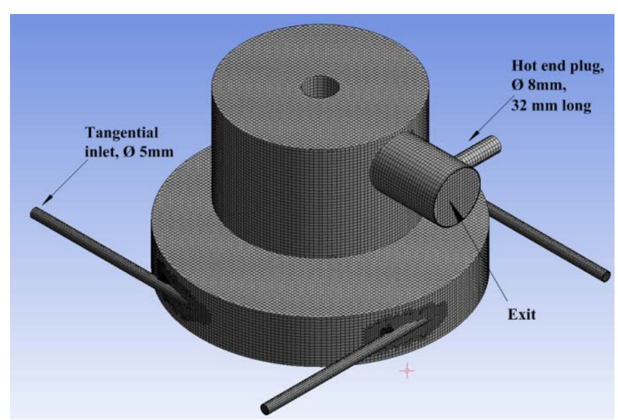

(a) Schematic of vortex chamber

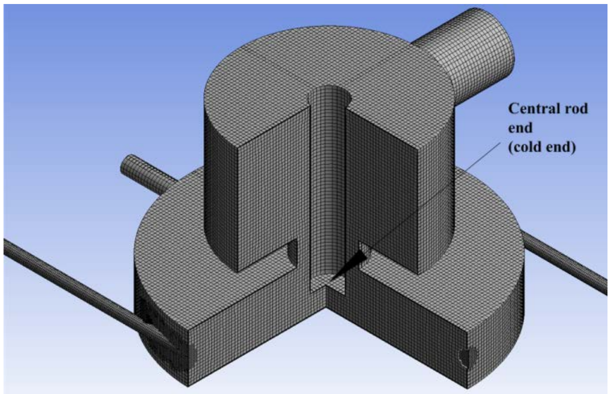

(b) Schematic cut-away view of vortex chamber

Figure 2 Computational mesh for the vortex chamber

VALIDATION

The present CFD model is validated with the pressure variation obtained from our resent experimental work [9]. The CFD simulations temperatures are measured at three radial locations (25mm, 50mm and 70mm) and inside the cavity (hottest point) and the bottom of the central rod (coldest point). Comparisons of the CFD results with the experimental values show a good agreement and reasonably predicted the radial pressure variation.

Figure 3 shows the comparison of the experimental and computational results for pressure inside the vortex chamber at an inlet pressure ratio (P/P_o) of 4. The calculated pressure values are in close agreement with the measured values at the center of the vortex chamber. With increase in the radial distance there are some differences between the calculated and measured values. However, the trend observed in the pressure variation is almost similar for the computational and experimental results.

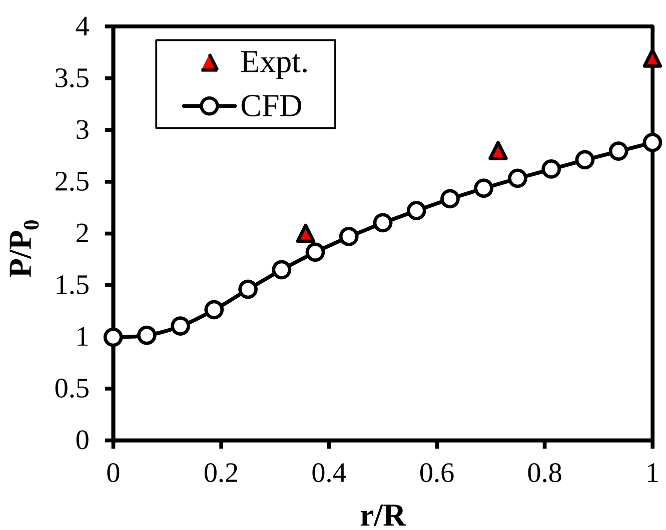

Figure 3 Comparison of CFD results with the radial experimental pressure variation [inside the vortex chamber for an inlet pressure ratio of 4.0.

EXPERIMENTAL RESULTS

Figure 4 shows that the amount of temperature separation is depended on the input pressure. With pressure ratio, T_i, T_{70}, T_{50}, and T_{25} increases, whereas T_c decreases. For an inlet pressure of ratio of 4.0 the following temperature ratios values were reached (high temperature): at a point T_i 1.116; at a point 50 mm from the center 1.114; and at a point 25mm from the center 1.092; and at center (T_c) 0.941 (low temperature). Hence, the present CFD model accounts for the temperature separation inside the vortex chamber very well. Moreover, the temperature inside the cavity (T_i) is remarkably higher than the vortex chamber surface temperature ($T_{70} = T_s$).

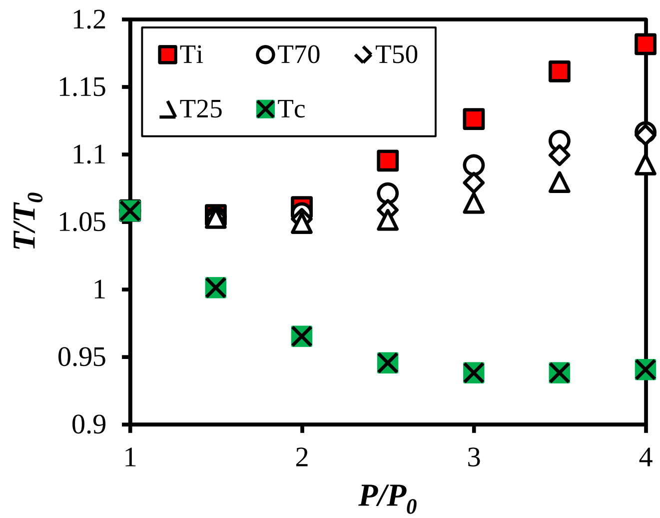

Figure 4 Temperature separation phenomenon inside the vortex chamber with different inlet pressure ratios.

NUMERICAL RESULTS

The temperature variations inside the cavity are shown by the mean static temperature variations obtained by the time averaging from the CFD in Fig. 5. It can be clearly seen that the temperature variation inside the cavity is sufficiently higher (about 25^0C). In addition, along the periphery of the vortex chamber the temperature is low. It was found that the energy separation mechanism in the vortex tube consists of three major processes. They are (1) adiabatic expansion at the tangential inlet nozzles, producing the lowest temperature in the system, (2) formation of a forced vortex (characterized by an increasing tangential velocity for increasing values of the radius) resulting in radial temperature gradients (due to viscous dissipation) and (3) the high-temperature separation inside the cavity.

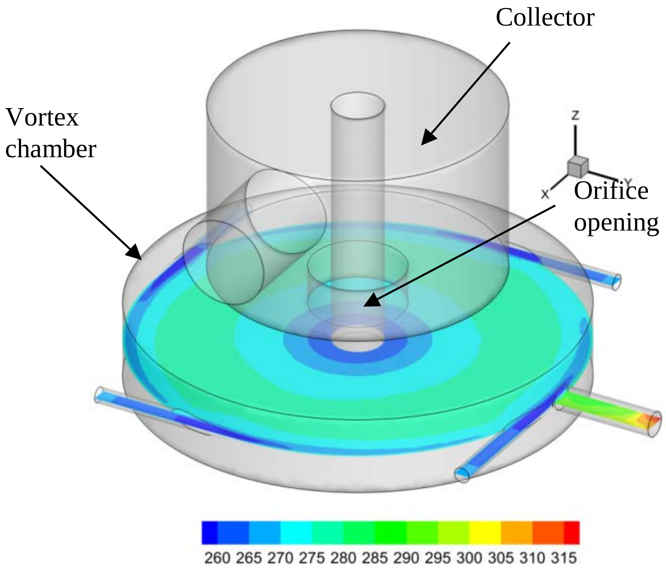

(a) horizontal section plane

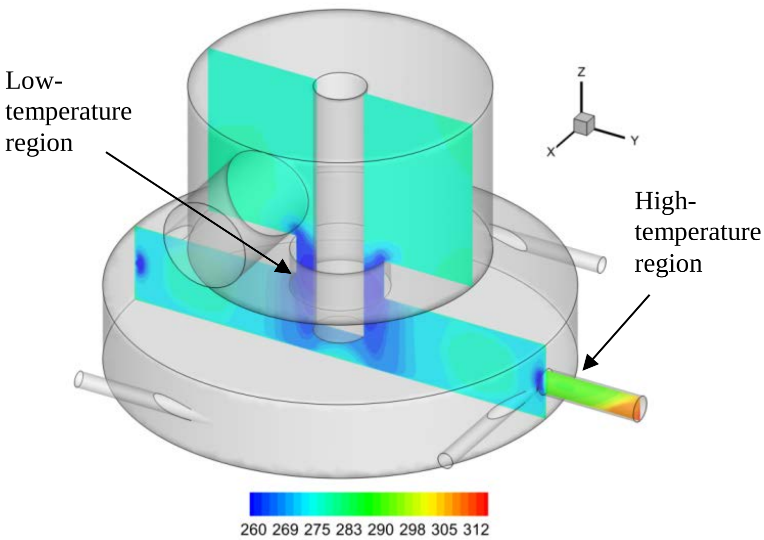

(b) vertical section plane

Figure 5 Time averaged mean static temperature contours on (a) horizontal section plane passing through bottom of the central-rod (cold-end, Z=0) (b) vertical section plane

A secondary flow field that forms a counter-rotating vortex with the primary flow has been observed within the vortex chamber (Fig. 7). The presence of this secondary flow field contributes to the energy migration by providing a frictional coupling between the two vortices resulting in a migration of energy to the cavity via shear work. Without the cavity such high temperatures are difficult to obtain with the present vortex-chamber geometry.

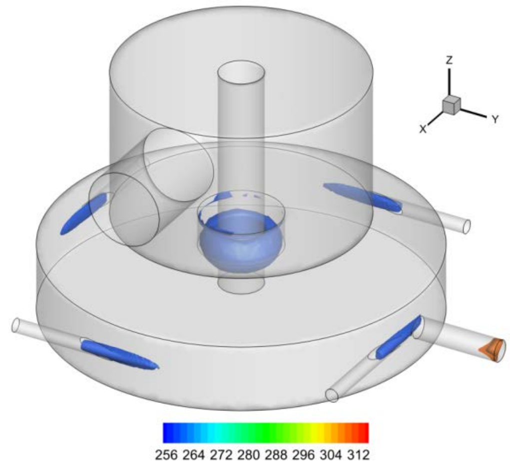

Figure 6 Low and high temperature separation areas inside the vortex chamber (Iso-surfaces of 260K and 310K are shown coloured by the time averaged static temperature).

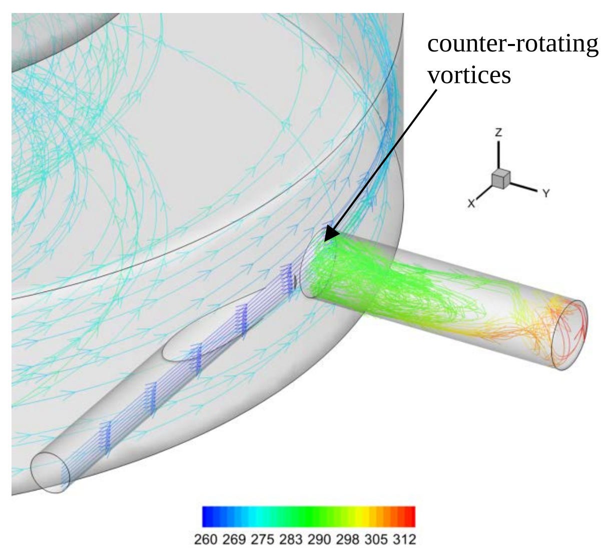

Figure 7 Counter-rotating vortices as a possible cause for the high-temperature separation inside the cavity.

The tangential injection of air into the vortex chamber creates high angular momentum inside the chamber. Due to the small orifice opening connecting the vortex chamber to the collector, only the outer portion of the vortex is allowed to escape through the orifice. The remainder of the gas is forced to return (due to the presence of the central-rod) forming an inner vortex of reduced diameter within the outer vortex (Fig. 8). Both vortices rotate in the same direction, but with reduced angular momentum for the inner vortex. The reduction in angular momentum is transferred as kinetic energy to the outer vortex, resulting in the formation of low-temperature inner-vortex.

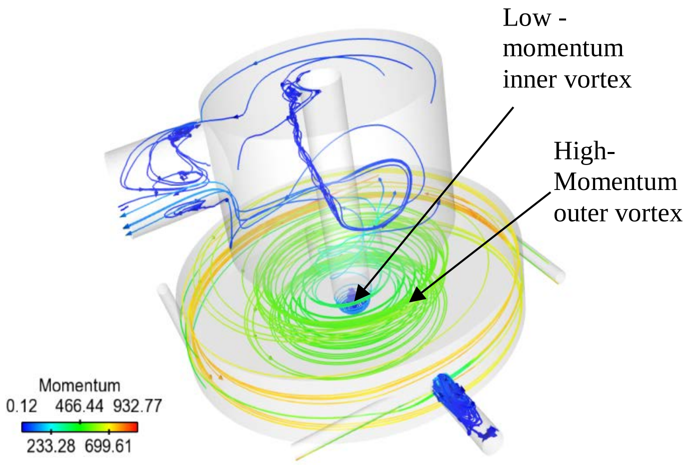

Figure 8 Formation of two distinct vortices inside the vortex chamber from a single compressed gas as a possible cause for low-temperature separation.

CONCLUSION

The possible reasons for the high and low temperature separation inside a vortex chamber are investigated in detail by the visualization of air flow. The distribution of the angular momentum indicates energy migration inside the vortex chamber. It is found that two vortices that rotate in the same direction are responsible for the low-temperature separation while counter-rotating vortices cause high-temperature separation.

Generally, RHVT is more efficient as a cooling device and vortex chamber is more suited as an air heater depending upon the configuration of the hot-end plug/cavity. For present vortex chamber geometry, high temperature separation is impossible to obtain without the cavity. The high-temperature separation is strongly depending on the configuration of this cavity. Further studies are planned to find the relationship between cavity geometry and the high-temperature separation for the vortex chamber.

REFERENCES

[1] G. J. Ranque, Experiments on Expansion in a Vortex with Simultaneous Exhaust of Hot Air and Cold Air, *J. Phys. Radium(Paris)*, Vol. 4, 1933, pp.1125-1130

[2] R. Hilsch, The use of the Expansion of Gases in a Centrifugal Field as Cooling Process, *Rev. Sci. Instrum.*, Vol. 18, No. 2, 1947, pp.108-113

[3] Yan Beliavsky, Experimental Investigation of a Temperature Separation Effect Inside a Short Vortex Chamber, *9th International Conference on Heat Transfer, Fluid Mechanics and Thermodynamics*, Malta, 2012.

[4] Yan Beliavsky, The Pressure Gradient Elastic Wave : Energy Transfer Process for Compressible Fluid with Pressure Gradient, *Journal of Engineering and Automation*, Vol. 3, 2013, pp. 53-64

[5] W. Frohlingsdorf and H. Unger, Numerical Investigations of the Compressible Flow and the Energy Separation in the Ranque–Hilsch Vortex Tube, *Int. J. Heat Mass Transfer* , Vol. 42, 1999, pp.415-422.

[6] U. Behera, P.J. Paul, K. Dinesh and S. Jacob, Numerical Investigations on Flow Behaviour and Energy Separation in Ranque–Hilsch Vortex Tube, *Int. J. Heat Mass Transfer*, Vol. 51, 2008, pp.6077-6089.

[7] Y. Xue, M. Arjomandi and R. Kelso, A critical review of temperature separation in a vortex tube, *Experimental Thermal and Fluid Science*, Vol. 34, 2010, pp.1367-1374.

[8] C.M. Gao, K.J. Bosschaart, J.C.H. Zeegers and A. Waele, Experimental study on a simple Ranque–Hilsch vortex tube, *Cryogenics*, Vol. 45, No. 3, 2005, pp.173-183.

[9] K. Yokoo, S. Matsuo, Y. Matsuno, T. Setoguchi and H.D. Kim, Flow Characteristic in a Vortex Chamber, *JMST*, 2014 (in Japanese)